THE JOURNAL OF BIOLOGICAL CHEMISTRY
Vol. 277, No. 48, Issue of November 29, pp. 46456–46462, 2002

Printed in U.S.A.

Purification and Properties of TrwB, a Hexameric, ATP-binding Integral Membrane Protein Essential for R388 Plasmid Conjugation*

Received for publication, July 19, 2002, and in revised form, September 12, 2002
Published, JBC Papers in Press, September 18, 2002, DOI 10.1074/jbc.M207250200

Itsaso Hormaeche‡§¶, Itziar Alkorta‡§, Fernando Moro‡, José M. Valpuesta‖, Félix M. Goñi‡, and Fernando de la Cruz‡‡**

From the ‡Unidad de Biofísica (Centro Mixto Consejo Superior de Investigaciones Científicas-Universidad del País Vasco and Departamento de Bioquímica, Universidad del País Vasco/Euskal Herriko Unibertsitatea, Apdo. 644, 48080 Bilbao, Spain, ‖Centro Nacional de Biotecnología, Consejo Superior de Investigaciones Científicas, Campus de Cantoblanco-Universidad Autónoma de Madrid, 28049 Madrid, Spain, and ‡‡Departamento de Biología Molecular (Unidad Asociada al Centro de Investigaciones Biológicas, CSIC), Universidad de Cantabria, C/Herrera Oria s/n, 39011 Santander, Spain

TrwB is an integral membrane protein linking the relaxosome to the DNA transport apparatus in plasmid R388 conjugation. Native TrwB has been purified in monomeric and hexameric forms, in the presence of dodecylmaltoside from overexpressing bacterial cells. A truncated protein (TrwBΔN70) that lacked the transmembrane domain could be purified only in the monomeric form. Electron microscopy images revealed the hexameric structure and were in fact superimposable to the previously published atomic structure for TrwBΔN70. In addition, the electron micrographs showed an appendix, ~25 Å wide, corresponding to the transmembrane region of TrwB. TrwB was located in the bacterial inner membrane in agreement with its proposed coupling role. Purified TrwB hexamers and monomers bound tightly the fluorescent ATP analogue TNP-ATP. A mutant in the Walker A motif, TrwB-K136T, was equally purified and found to bind TNP-ATP with a similar affinity to that of the wild type. However, the TNP-ATP affinity of TrwBΔN70 was significantly reduced in comparison with the TrwB hexamers. Competition experiments in which ATP was used to displace TNP-ATP gave an estimate of ATP binding by TrwB ($K_{d(ATP)}$ = 0.48 mM for hexamers). The transmembrane domain appears to be involved in TrwB protein hexamerization and also influences its nucleotide binding properties.

Bacterial conjugation is a highly efficient and broad host range process during which DNA is transferred from a donor to a recipient bacterium across the envelope of both cells (for reviews, see Refs. 1 and 2). Conjugative DNA transfer requires three sets of plasmid-encoded proteins called Dtr (DNA transfer and replication), Mpf (mating pair formation) (3), and a coupling protein (2, 4). Dtr proteins process conjugative DNA through the formation of a nucleoprotein complex, the relaxosome, that cleaves and unwinds DNA in order to form the single DNA to be transferred (T-strand). The relaxosome "moves" to the transport site by means of the coupling protein, where the DNA transport apparatus (Mpf proteins) provides the pore for transport of the T-strand to the recipient cell (2, 4).

Plasmid R388 has the shortest known mobilization region (5, 6). Only three plasmid-encoded proteins, TrwA, TrwB, and TrwC, together with *oriT*, are involved in R388 mobilization (6). TrwC acts as a relaxase and a DNA helicase. It is responsible for both nick cleavage at *oriT* and T-strand unwinding (7, 8). TrwA is a small tetrameric protein, which binds two sites at *oriT* and enhances TrwC relaxase activity, while repressing transcription of the *trwABC* operon (9). The R388 relaxosome is composed of TrwA and TrwC bound to *oriT* DNA together with the host protein IHF. The latter inhibits TrwC *nic* cleavage by affecting the topology of the DNA site where TrwC has to act. By so doing, it is thought to modulate R388 conjugation (10).

The third plasmid-encoded protein necessary for R388 conjugative DNA processing is TrwB, which belongs to the coupling protein family. TrwB sequence analysis predicts an integral membrane protein of 507 residues (6, 11) and contains the characteristic NTP-binding motifs, reminiscent of those of the α and β subunits of F_1-ATPase (12, 13) and shared by the other coupling proteins (14). The transmembrane domain predicted by sequence analysis comprises the 70 N-proximal residues and includes two transmembrane helices and a small periplasmic domain in between. Although the coupling proteins appear to play an essential role in bacterial conjugation, few data are available on their biochemical mechanism. Protein TraD was the first coupling protein purified and subjected to biochemical analysis (15). Later, a soluble form of TrwB, lacking the N-terminal transmembrane segments and called TrwBΔN70, was purified (11) (see below). Recently, His-tagged TraG (RP4) and TraD (F) and truncated HP0524 (*Helicobacter pylori*) have been purified and partially characterized (16). Apparently, problems of aggregation and solubility precluded a more exhaustive characterization of these proteins. The poverty of results obtained *in vitro* underscores the difficulty in handling integral membrane proteins.

We observed that in the purification protocol, TrwBΔN70 behaved as a monomer. However, its crystal structure unveiled a molecule with six equivalent protein units (4). In this study, we have purified the integral membrane protein TrwB in its native form from an extract of TrwB-overproducing *Escherichia coli* cells. Unlike TrwBΔN70, TrwB appears in both monomeric and hexameric forms in solution. Since this behavior is different from the one corresponding to the TrwBΔN70 mutant, we infer that the transmembrane portion could play an important role in TrwB oligomerization. Our electron mi-

* This work was supported by Ministerio de Ciencia y Tecnología Grant BMC 2001.0791 and Universidad del País Vasco Grant 13552/2001. The costs of publication of this article were defrayed in part by the payment of page charges. This article must therefore be hereby marked "*advertisement*" in accordance with 18 U.S.C. Section 1734 solely to indicate this fact.

§ These two authors contributed equally to this work.
¶ A predoctoral fellow of MCYT.
** To whom correspondence should be addressed. E-mail: gbpgourf@lg.ehu.es.

TABLE I
E. coli strains and bacterial plasmids used in this work

Strain	Genotype	Reference
DH5α	F⁻ *endA1 hsdR17 supE44 thi-recA1 relA1* Δ(*argF-lacZYA*)U160 φ80d *lacZ* Δ *M15 gyrA96*	42
UB1637	F⁻ *lys his trp rpsL recA56*	43
BL21 (DE3)	F⁻ *ompT hsdS⁻ gal*(::DE3)	44
BL21C41(DE3)	F⁻ *ompT hsdS⁻ gal*(::DE3)	21
D1210	F⁻ *recA hsdR hsdM rpsL lacI^q*	45

Plasmid	Description	Phenotype[a]	Reference
pSU4743	Expression vector derived from pET3 by *Ssp*I/*Cla*I deletion	Ap^R, Rep(pMB8)	20
pSU24	Cloning vector	Cm^R, LacZα, Rep(p15A)	46
pHG327	Cloning vector	Ap^R, Rep(pMB8)	47
pSU1425	R388 without *Eco*R1 site	Su^R, Tp^R, TRA_w^+, IncW	48
pSU1456	pSU1425::Tn5Δ*Eco*RI	Su^R, Tp^R, Mob^-, IncW	48
pSU4051	pHG327::MOBW	Ap^R, Rep(pMB8)	5
pSU4623	pSU24::*trwA*+*trwB*	Cm^R, Rep(p15A)	11
pSU4632	pSU24::*trwA*+*trwB* K136T	Cm^R, Rep(p15A)	11
pBU1	pSU4743::*trw*B	Ap^R, Rep(pMB8)	This work
pBU2	pSU4743::*trw*B K136T	Ap^R, Rep(pMB8)	This work
R388	Wild type plasmid	Su^R, Tp^R, TRA_w^+, IncW	49

[a] Ap, Cm, Su, and Tp, resistance to ampicillin, chloramphenicol, sulfonamides, and trimethoprim, respectively. Rep indicates the type of replicon (in parentheses).

croscopy results support this theory and corroborate the TrwBΔN70 tridimensional structure. Moreover, hexameric TrwB has been found to bind ATP with a dissociation constant of ~0.5 mM (*i.e.* in the order of magnitude of other ATP-binding proteins) (17–19).

MATERIALS AND METHODS

Bacterial Strains and Plasmids—E. coli strains are described at the top of Table I, and plasmids are listed at the bottom. For conjugation experiments, the recA strains DH5α and UB1637 were used as donor and recipient strains, respectively.

Oligonucleotides and Construction of Plasmids pBU1 and pBU2—The oligonucleotides used in the present work were 1) GAAGGAGGATTCATATGCATCCAGA, which creates an *Nde*I site (underlined) and start codon at the N terminus of the *trwB* gene, 2) GATTTACCGGTACCAGT, which creates a *Kpn*I site (underlined) at nucleotides 398–403 of the *trwB* gene, and 3) GCAACACCGAGGTACCCGTACC, which creates a *Kpn*I site (underlined) at nucleotides 404–409 of the *trwB* gene and a K136T mutation in TrwB protein.

In order to overproduce TrwB protein, plasmid pBU1 was constructed as follows. Plasmid pSU4623, which carries the *trwB* gene with a silent mutation to create a *Kpn*I site (11), was used as template for a PCR with oligonucleotides 1 and 2 (see above). The resulting 423-bp fragment was digested with *Nde*I and *Kpn*I (fragment 1). Simultaneously, pSU4623 was digested with *Kpn*I and *Bam*HI, the resulting 1.1-kb fragment was mixed with fragment 1, and this mixture was cloned in *Nde*I-*Bam*HI-digested pSU4743 (pET-3a derivative) (20). This resulting construction contains TrwB protein under the control of the T7 promoter. Plasmid pBU1 was transformed to and stored in strain D1210. For protein overproduction, plasmid pBU1 was introduced in *E. coli* BL21 C41 (DE3), a mutant strain of *E. coli* BL21 (DE3) (21). To overproduce TrwB-K136T, plasmid pBU2 was constructed as described before, and pSU4632 plasmid that carries the *trwBK136T* gene where the K136T mutation creates a *Kpn*I site was used (11). In the latter case, oligonucleotides 1 and 3 (see above) were used for PCR.

TrwB Purification—TrwB was routinely purified from induced *E. coli* BL21 C41 (DE3) cells. Cultures (6 × 500 ml of LB with 0.1 mg/ml ampicillin) of *E. coli* BL21 C41(DE3) harboring the plasmid pUB1 were grown at 37 °C with shaking. At an A_{550} of 0.6–0.8, isopropyl β-D−thiogalactopyranoside was added to a concentration of 1 mM. Cells were grown at 25 °C for 3 h. The cultures were centrifuged at 11,000 × *g* for 15 min; the cells were then resuspended in the remaining volume of LB and frozen in liquid N_2. Frozen cells were thawed at 37 °C in 30 ml of buffer A (50 mM Tris-HCl (pH 7.8), 0.1 mM EDTA, 200 mM NaCl) containing 1 mM dithiothreitol, 1 mM phenylmethylsulfonyl fluoride, and 0.07% (w/v) of lysozyme. After 30 min at 0 °C, the cells were disrupted by sonication (10 s on/10 s off, 30 cycles) and centrifuged at 7000 × *g* for 15 min to sediment the nonlysed cells. The supernatant was centrifuged at 100,000 × *g* for 1 h at 4 °C, and the pellet that constitutes the membrane fraction was resuspended in 15 ml of buffer A. For protein solubilization, membranes were treated with β-D-dodecylmaltoside (Apollo, Waley Bridge, Derbyshire, UK) and NaCl to a final concentration of 1% (w/v) and 600 mM, respectively. The membrane preparation (30 ml) was incubated for 2 h at 4 °C with continuous stirring and then centrifuged at 100,000 × *g* for 1 h. TrwB was recovered from the supernatant (Fraction I, 30 ml) (Fig. 1).

Fraction I was brought to 200 mM NaCl by the addition of buffer B (50 mM Tris-HCl (pH 7.8), 0.1 mM EDTA, 0.05% β-D-dodecylmaltoside) and applied at 1 ml/min to a 40 ml of cellulose phosphate P-11 (Whatman) column (2.5 × 8 cm) equilibrated with buffer B supplemented with 200 mM NaCl. Proteins were eluted in two steps: 500 mM NaCl in buffer B (fraction II, 100 ml) and 1 M NaCl in buffer B (fraction II′, 50 ml). TrwB eluted in both steps. From this point on, fractions II and II′ followed separate, although parallel, purification protocols.

Fraction II′ was diluted to 150 mM NaCl by the addition of buffer B and loaded onto a 5-ml HiTrap-SP (Amersham Biosciences) column connected to an Amersham Biosciences FPLC[1] system equilibrated with buffer B containing 150 mM NaCl. The column was washed with this buffer B until base line was reached. Proteins were then eluted from the column with a 150–1000 mM NaCl gradient in buffer B at a flow rate of 2.5 ml/min. TrwB, as a monomer, eluted at about 275 mM NaCl (Fraction III′-m, 30 ml), and the hexameric form eluted at about 710 mM NaCl (Fraction III′-h, 75 ml). Fraction III′-m was concentrated by Centriprep and Centricon YM-50 systems (Amicon) to a final volume of 5 ml and loaded onto a 120-ml Superdex HR 200 column (16 × 60 cm) (Amersham Biosciences) by using Amersham Biosciences FPLC equipment. Gel filtration was performed in buffer B with 200 mM NaCl at a flow rate of 0.5 ml/min. The peak fractions corresponding to the monomer were pooled (fraction IV′-m, 10 ml), and after glycerol was added to a 20% (w/v) final concentration, they were stored at −80 °C. Similarly, fraction III′-h was concentrated by Centriprep and Centricon YM-50 systems (Amicon) to a final volume of 250 μl and loaded onto a 24-ml Superose 6 column (10 × 30 cm) (Amersham Biosciences) by using FPLC equipment. Gel filtration was performed in buffer B with 200 mM NaCl at a flow rate of 0.25 ml/min. The peak fractions corresponding to the hexamer were pooled (fraction IV′-h, 4.4 ml), glycerol was added to a 20% (w/v) final concentration, and the protein was stored at −80 °C.

Fraction II was treated exactly as fraction II′ through the HiTrap-SP and Superdex HR-200, giving rise to a single, monomeric fraction IV (Fig. 1). The TrwB-K136T mutant protein was purified following the same purification protocol.

All protein determinations were performed by the BCA method (Pierce).

Production of Antibodies—Anti-TrwB protein polyclonal antibodies were prepared using the method described by Harlow and Lane (22). For antibody production, TrwB was purified by preparative SDS gel electrophoresis of a membrane fraction solubilized with Triton X-100 (1%, w/v) and applied first onto a DE52 (Whatman) column and then to a HiTrap Heparin (Amersham Biosciences) column. The band corre-

[1] The abbreviations used are: FPLC, fast protein liquid chromatography; TNP-ATP, 2′(or 3′)-*O*-(2,4,6-trinitrophenyl)adenosine 5′-triphosphate.

sponding to the TrwB protein was cut out of the gel and used to immunize New Zealand White rabbits. The IgG fraction from the serum was purified by chromatography on a Protein A-Sepharose column.

Cellular Localization of TrwB Protein—Separation of the inner (cytoplasmic) and outer membranes was carried out essentially as described by Osborn and Munson (23). Cells were grown to exponential phase and then harvested. Cell pellets were resuspended in 10 mM Tris-HCl (pH 7.8), containing 1 mM EDTA, 1 mM dithiothreitol, 0.75 M sucrose, and 0.1 mg/ml lysozyme. Then spheroplasts were formed by dilution with 2 volumes of 1.5 mM EDTA and lysed by brief sonication. The total membrane fraction was obtained by ultracentrifugation and resuspension in 5 mM EDTA (pH 7.5) supplemented with 20% sucrose. Outer and inner membrane fractions were prepared by loading the total membrane fraction on a continuous sucrose density gradient from 34 to 70% and then centrifuging at 96,000 × *g* for 16 h at 4 °C (Beckman rotor TST 28.38). Membrane fractions were identified through determination of specific activities as ketodeoxyoctonate and NADH oxidase for outer and inner membrane, respectively.

Genetic Techniques—Bacterial transformation with plasmid DNA was carried out by the $CaCl_2$ method (24). Genetic complementation analysis of the conjugal ability of TrwB was carried out as described by Llosa *et al.* (6). Donor cells were selected on Tp + Ap, and transconjugants were selected on Sm + Tp.

Electron Microscopy and Image Processing—Aliquots of TrwB were applied to carbon grids, negatively stained with 2% uranyl acetate. Images were taken in a JEOL 1200EX-II electron microscope operated at 100 kV and recorded on Kodak SO-163 film at 60,000× nominal magnification. Micrographs were digitized at a 3.5 Å/pixel resolution using a Eikonix IEEE-488 camera. 860 side view particles and 530 top view particles of TrwB were extracted and aligned by cross-correlation free-pattern methods (25), and processed using the XMIPP package (26). Resolution of the final average images of both side and top views was estimated by the spectral signal/noise ratio method (27) to be 25 and 27 Å, respectively.

Nucleotide Binding—The nucleotide binding properties of TrwB were studied using a fluorescent ATP analogue, namely TNP-ATP (Molecular Probes, Inc., Eugene, OR) (28). Experiments were performed at 25 °C using a PerkinElmer MPF-66 spectrofluorometer, with spectral bandwidths of 5 and 10 nm for excitation and emission, respectively. Proteins were suspended in buffer A supplemented with 0.05% (w/v) β-D-dodecylmaltoside and 20% (w/v) glycerol. All spectra were corrected for buffer fluorescence and for dilution (never exceeding 5% of the original volume). When the extrinsic fluorescence of TNP-ATP was studied, excitation was performed at 410 nm, and emission was scanned in the 470–650-nm range. TNP-ATP binding was determined from the increase in fluorescence at 560 nm in the presence of TrwB protein (29). Titration curve fitting was accomplished using SigmaPlot 2001 for Windows, Version 7.0 (SPSS Inc.) with the following quadratic equation in the case of increasing TNP-ATP fluorescence,

$$F = F_{min} + \{(F_{max} - F_{min})[(E_t + L + K_{d(TNP\text{-}ATP)}) - ((E_t + L + K_{d(TNP\text{-}ATP)})^2 - 4E_tL)^{1/2}]\}/2E_t \quad \text{(Eq. 1)}$$

where F represents the relative fluorescence intensity, F_{min} is the relative fluorescence intensity at the start of titration, F_{max} is the fluorescence intensity at saturating concentration of TNP-ATP (L), E_t is the total concentration of TrwB, and $K_{d(TNP\text{-}ATP)}$ is the apparent dissociation constant of TrwB-substrate complex.

In the case of displacement of bound TNP-ATP by ATP, the following quadratic equation was used,

$$F = F_{max} - \{(F_{max} - F_{min})[(E_t + L + K_{0.5}) - ((E_t + L + K_{0.5})^2 - 4E_tL)^{1/2}]\}/2E_t \quad \text{(Eq. 2)}$$

were F_{max} is the fluorescence intensity at start of the titration, and F_{min} is the fluorescence at saturating concentration of ATP, $K_{0.5}$ in this equation represents the amount of ATP necessary to displace half the amount of bound TNP-ATP, and L represents ATP concentrations. Therefore, it is possible to calculate the apparent dissociation constant of TrwB-ATP complex ($K_{d(ATP)}$) by using the $K_{0.5}$ value obtained from the displacement experiments and the following equation,

$$K_{d(ATP)} = K_{0.5}/\{1 + [L/K_{d(TNP\text{-}ATP)}]\} \quad \text{(Eq. 3)}$$

where L represents TNP-ATP concentration at start of the titration.

RESULTS

TrwB Purification—The purification scheme of TrwB is shown in Fig. 1 and described under "Materials and Methods." We have purified TrwB to apparent homogeneity from extracts of *Escherichia coli* BL21 C41 (DE3) carrying the *trwB* gene on a multicopy plasmid derived from pET3a. After induction with 1 mM β-D−thiogalactopyranoside, cells were grown at 25 °C to avoid formation of inclusion bodies and to promote integration of the protein into the cytoplasmic membrane. Membrane integration at this stage helped in obtaining functionally active protein.

Cells were harvested and membranes were obtained after breaking cells by sonication and subsequent centrifugation. After centrifugation, the following detergents were tested for TrwB solubilization: 1) 50 or 100 mM octyl glucoside; 2) 40 or 200 mM CHAPS; 3) 1% (w/v) Triton X-100; 4) 56 mM sodium cholate; 5) 1% (w/v) β-D-dodecylmaltoside. β-D-Dodecylmaltoside was the most effective in extracting TrwB from the membranes (data not shown). Furthermore, it was found that the addition of 600 mM NaCl improved protein solubilization.

Solubilized membranes were chromatographed on a cellulose phosphate P-11 column from which two fractions were obtained, at low (fraction II) and high (fraction II′) salt concentrations, respectively. These two fractions were separately treated from this stage onwards (see *A* and *B*, respectively, in Fig. 2). Fraction II (Fig. 2*A*, *lane 2*) was applied to a HiTrap-SP column and finally sieved on Superdex HR-200 where TrwB eluted to give 3.83 mg of homogeneous TrwB monomer (Fig. 2*A*, *lane 4*).

Fraction II′ was applied to a HiTrap-SP column, and the resulting subfractions III′-m and III′-h were respectively applied to a Superdex HR-200 column, to give 0.5 mg of homogeneous TrwB monomer (Fig. 2*B*, *lane 4*) and to a Superose-6 column to give 0.34 mg of homogeneous TrwB hexamer (Fig. 2*B*, *lane 6*).

The TrwB-K136T mutant protein was purified following the same purification protocol. However, the protein yield was strongly reduced in all fractions, and consequently only fraction II was obtained in significant amounts at the end of the purification. Thus, the studies involving the mutant protein were carried out with monomeric TrwB-K136T only. Note, however, that, although in small amounts, a fraction II′ of the mutant protein was obtained that, when processed through the HiTrap-SP column, could be resolved into monomers and hexamers (data not shown).

Cellular Localization—We examined the localization of TrwB by using specific antibody detection. *E. coli* D1210 cells containing the R388 plasmid were grown to exponential phase and lysed as described under "Materials and Methods." Membrane fractions were prepared, and proteins were separated by SDS-PAGE. After immunoblotting, TrwB protein was specifically found in the inner membrane fractions of D1210 cells containing the R388 plasmid (Fig. 3). This result is fully compatible with the putative function of TrwB as a connector of the relaxosome (in the cytoplasm) to the transport system (in the membrane).

Electron Microscopy of TrwB—Samples of TrwB fraction IV′-h were visualized by electron microscopy. Two preferred orientations of TrwB could be observed. The most abundant one can be defined as the side view (Fig. 4, *upper panel A*), and the processing of 860 of such particles generated an average image (Fig. 4, *lower panel A*) that was similar, albeit to a different resolution, to the lateral projection of the atomic structure of the TrwBΔN70 (Fig. 4, *lower panel B*), a mutant in which the first 70 residues, putatively involved in forming the membrane pore, have been deleted (30). Both projections

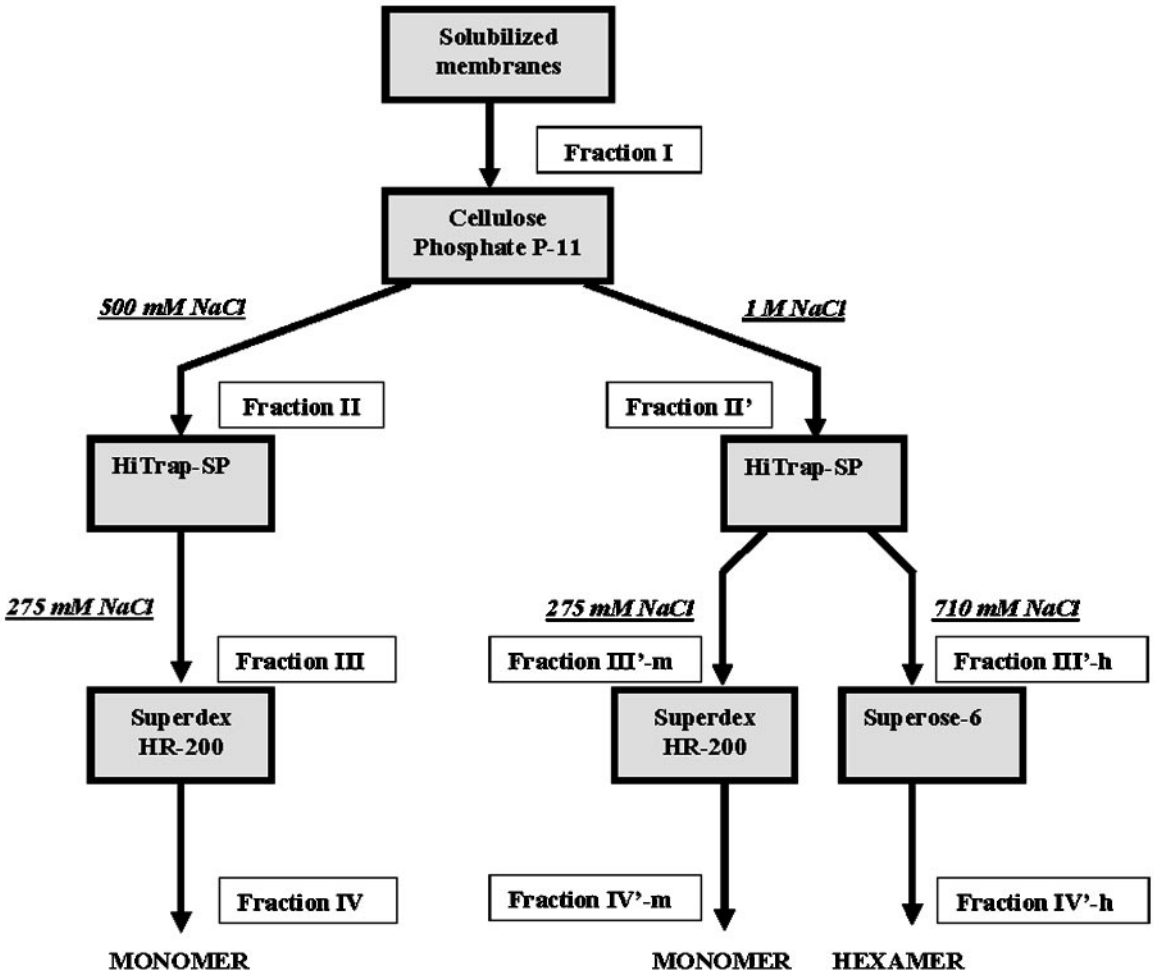

FIG. 1. **Purification scheme of TrwB.** See "Materials and Methods" for further details.

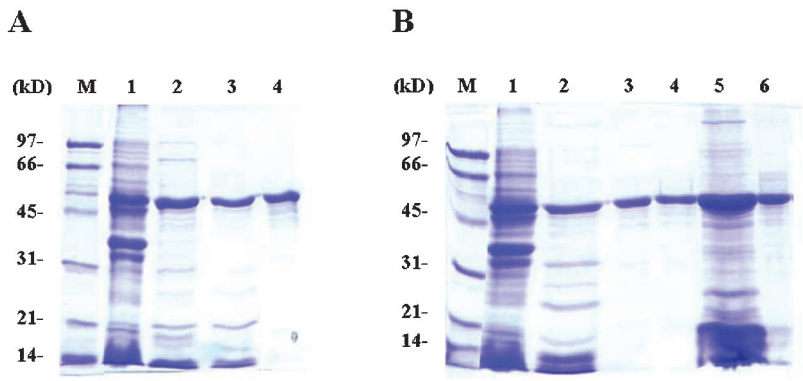

FIG. 2. **Purification of TrwB monomers and hexamers.** Proteins at each purification step were electrophoresed in 10% SDS-PAGE and stained with Coomassie Brilliant Blue. *A*, *lane 1*, solubilized membranes (fraction I) (48 mg of protein); *lane 2*, cellulose phosphate P-11 500 M NaCl eluate (fraction II) (10 mg); *lane 3*, HiTrap-SP chromatography (fraction III) (10 mg); *lane 4*, pool after applying fraction III onto a Superdex HR-200 column (fraction IV) (2.5 mg). *Lane M*, marker proteins. *B*, *lane 1*, solubilized membranes (fraction I) (48 mg of protein); *lane 2*, cellulose phosphate P-11, 1 M NaCl eluate (fraction II′) (10 mg); *lane 3*, HiTrap-SP 275 mM NaCl eluate (fraction III′-m) (3 mg); *lane 4*, pool after applying fraction III′-m onto a Superdex HR-200 column (fraction IV′-m) (2.5 mg); *lane 5*, HiTrap-SP 700 mM NaCl eluate (fraction III′-h) (27.3 mg); *lane 6*, pool after applying fraction III′-h onto a Superose-6 column (fraction IV′-h) (2.3 mg). *Lane M*, marker proteins.

shared similar features, an orange-shaped structure with a channel traversing its central part. An important difference between both structures resides nevertheless in an ~25-Å-wide appendix located at the bottom of the wild-type TrwB, which can be correlated with the transmembrane region of the protein and was not present in the structure of TrwBΔN70. This region was not as well resolved as the major domain, and this may be due to the presence of detergent shielding its hydrophobic core. The wider amplitude of the bottom of the transmembrane domain (Fig. 4, *lower panel A*) may be due to its intrinsic flexibility, which generates a blurring of this region in the average image. The other preferred orientation of TrwB can be defined as the *top view* (Fig. 4, *upper panel B*). The average image of 530 of these particles (Fig. 4, *lower panel C*) revealed a structure similar to the projection of the atomic structure of the TrwBΔN70 mutant along its 6-fold axis (Fig. 4, *lower panel D*). This average image presents, as its atomic counterpart, a central channel and six masses surrounding it, which undoubtedly

indicates that TrwB was purified as a hexamer.

Nucleotide Binding to TrwB—Upon protein binding, the fluorescence emission intensity of the fluorescent ATP analogue TNP-ATP (28) increases considerably; thus, it has been widely used to characterize ATP binding by a number of proteins (19, 31–36). As reported previously, TrwBΔN70 binds TNP-ATP as expected from the NTP binding signature in its amino acid sequence (11). Consequently, in this work, we used fluorescence spectroscopy to monitor the interaction of TNP-ATP with both TrwB and TrwB-K136T. The fluorescence emission spectrum of TNP-ATP in the presence of TrwB hexamers (Fig. 5) indicated a remarkable enhancement of the emission intensity and a blue shift (from 552 to 546 nm) of the wavelength of maximal emission. These were both indications that TNP-ATP had been transferred from the aqueous medium to the less polar environment inside the protein. Qualitatively similar spectra were obtained when monomeric TrwB was used (data not shown).

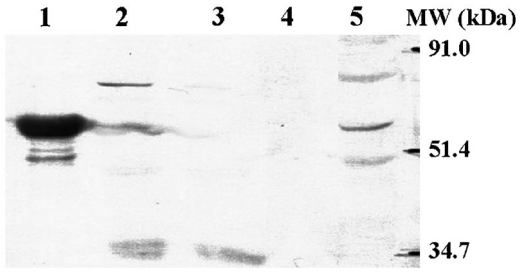

FIG. 3. **Localization of TrwB protein.** Inner and outer membrane fractions were separated by sucrose gradient centrifugation as described under "Materials and Methods." Samples of the different fractions were run on a 10% SDS-polyacrylamide gel that subsequently was subjected to immunoblotting with anti-TrwB IgGs. *E. coli* D1210 cells containing R388 plasmid. *Lanes 2–5*, cell extract, cytoplasmic, outer membrane, and inner membrane fractions, respectively. *Lane 1*, purified TrwB was used as control.

When TrwB was titrated with increasing amounts of TNP-ATP in the micromolar range, the relative increase in fluorescence became saturated, as seen in Fig. 6, for TrwB hexamers and monomers. This is the behavior expected for ATP-binding proteins (17, 18, 36–38). Our experimental results fitted well the saturation curves described by Equation 1, from which apparent dissociation constants for TNP-ATP ($K_{d(\text{TNP-ATP})}$) could be computed. The corresponding values for TrwB hexamers and monomers were of 1.18 ± 0.38 and 2.35 ± 0.45 μM, respectively. These values should be compared with the $K_{d(\text{TNP-ATP})}$ = 9.2 μM observed for the truncated TrwBΔN70 (11).

The TNP-ATP binding has two components: specific binding to the ATP-binding site and nonspecific binding of the TNP moiety to nonpolar residues in the vicinity of the ATP-binding site (28). The nonspecific component can be eliminated by add-

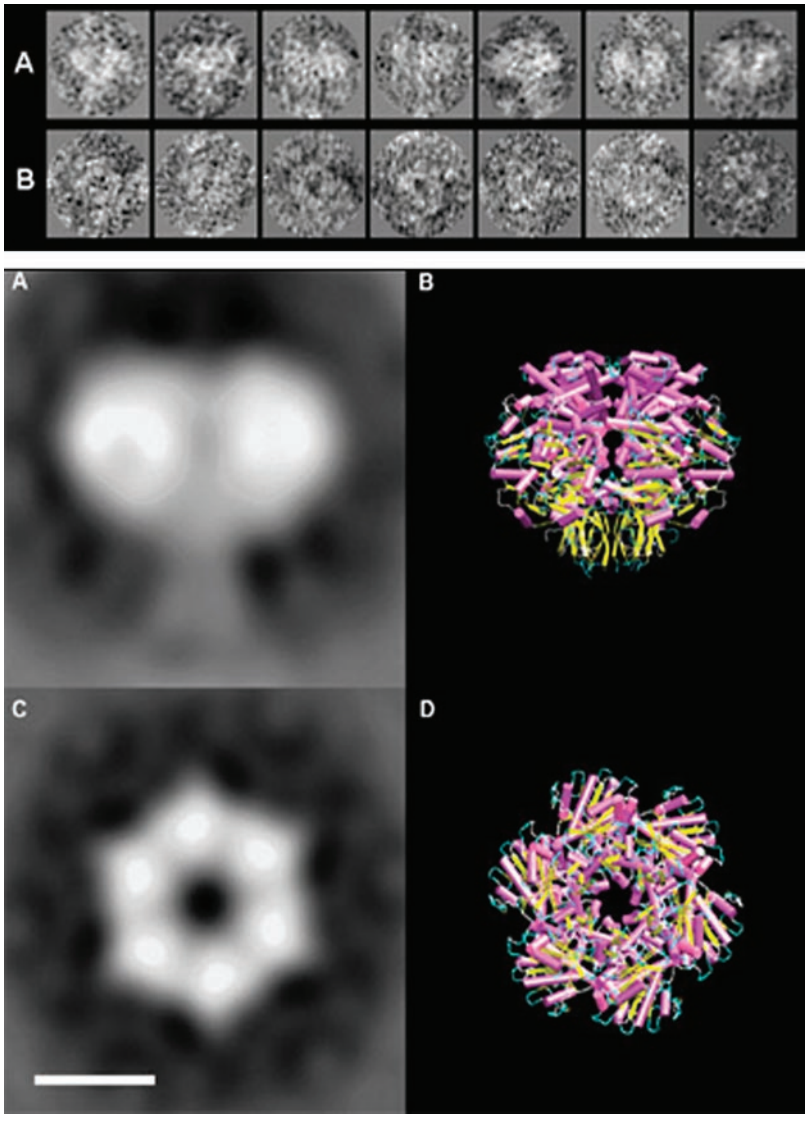

FIG. 4. *Upper panel*, gallery of negatively stained images of TrwB. *A*, gallery of side views. *B*, gallery of top views. *Lower panel*, two-dimensional negatively stained average images of the TrwB oligomer. *A* and *C*, average images of the side view and top view of TrwB, respectively. *B* and *D*, side and top projections, respectively, of the atomic structure of TrwBΔN70 mutant, to which the first 70 residues have been deleted (Protein Data Bank access code 1e9s) (30). All four images are shown at the same magnification. *Bar*, 50 Å.

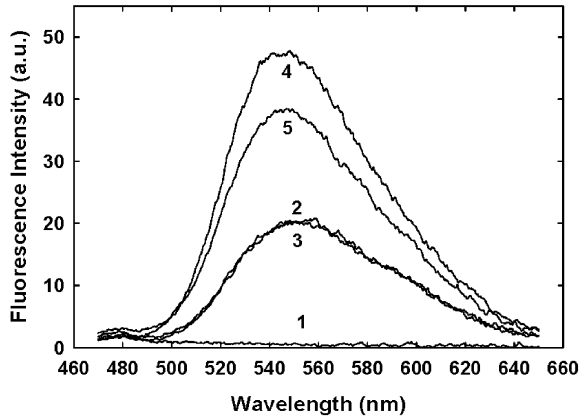

FIG. 5. **Fluorescence spectra of TrwB-bound TNP-ATP in the presence and absence of ATP.** Details of the experiment are described under "Materials and Methods." *Spectrum 1*, spectrum of TrwB hexamers (1 μM); *spectrum 2*, TNP-ATP (8 μM); *spectrum 3*, TNP-ATP (8 μM) plus ATP (5 mM); *spectrum 4*, TrwB hexamers (1 μM) plus TNP-ATP (8 μM); *spectrum 5*, TrwB hexamers (1 μM) plus TNP-ATP (8 μM) plus ATP (5 mM).

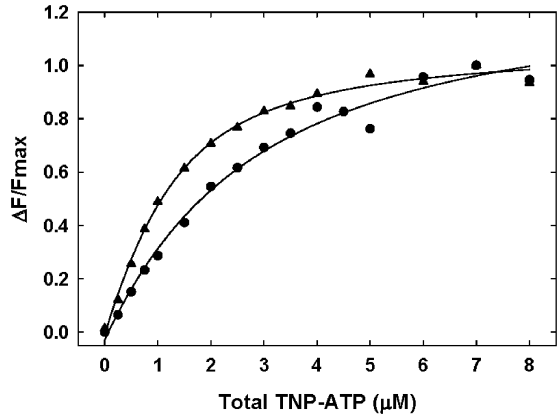

FIG. 6. **Fluorescence-monitored titration of TNP-ATP binding to TrwB protein.** Successive aliquots of TNP-ATP stock solutions were added to a 0.4-ml sample of TrwB hexamers (1 μM) (▲) or TrwB monomers (0.8 μM) (●), and the fluorescence intensity (excitation 410 nm, emission 560 nm) was recorded after each addition. Each plotted value represents the difference in fluorescence intensity between the TrwB tritration and the blank titration and was corrected as described under "Materials and Methods." The *lines* represent the best fit to the data generated using Equation 1.

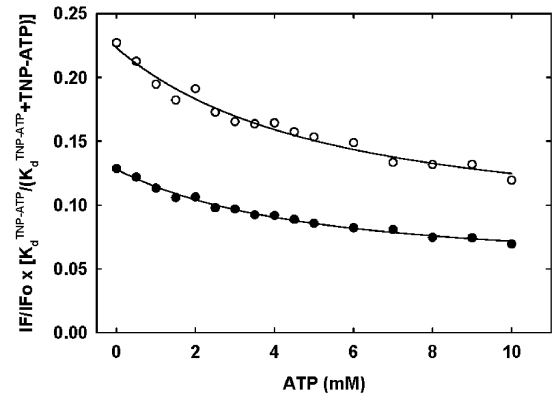

FIG. 7. **Displacement of bound TNP-ATP by ATP in TrwB hexamers.** Successive aliquots of ATP stock solutions were added to a solution containing TrwB hexamers (1 μM) (●) or TrwB monomers (0.8 μM) (○) and TNP-ATP (8 μM) in buffer A supplemented with 0.05% β-D-dodecylmaltoside and 20% glycerol. The fluorescence intensity (excitation 410 nm, emission 560 nm) was recorded after each addition. Each plotted value represents the difference in fluorescence intensity between the TrwB tritration and the blank titration and was corrected as described under "Materials and Methods." The *solid line* represents the best fit to the data generated using Equation 2.

ing excess ATP, which progressively removes TNP-ATP from the nonspecific binding sites. *Spectrum 5* in Fig. 5 corresponds to TrwB hexamer incubated with TNP-ATP and then with excess ATP. The nonfluorescent nucleotide induced a clear decrease in fluorescence. In this kind of experiment, ATP acts as a competitor ligand with respect to TNP-ATP. Proteins saturated with TNP-ATP could be thus back-titrated with ATP, as shown in Fig. 7. The experimental points fit very well a curve generated from Equation 2. Equation 2 allows an estimation of $K_{0.5}$ (*i.e.* the amount of ATP necessary to displace half the amount of bound TNP-ATP), and from $K_{0.5}$, Equation 3 allows computation of the apparent dissociation constant of the protein-ATP complex ($K_{d(\mathrm{ATP})}$) (39). From the results in Fig. 7, a $K_{d(\mathrm{ATP})}$ = 0.48 mM for TrwB hexamer was obtained. Similar studies performed with TrwB monomer provided a $K_{d(\mathrm{ATP})}$ = 1.20 mM, in agreement with the idea that the hexamer affinity for ATP is higher than that of the monomer. $K_{d(\mathrm{ATP})}$ values in the millimolar range of ATP concentrations are common in ATP-binding proteins (19, 40). The relatively small difference between the ATP-binding affinities of TrwB monomers and hexamers could be due to ATP-dependent hexamerization. However, electron microscopy observations failed to reveal any such effect of ATP. Cross-linking induced by disuccinimidyl suberate also did not show any difference between ATP-treated and control TrwB monomers when the cross-linked proteins were separated by gel electrophoresis (data not shown).

The mutant in the Walker A motif TrwB-K136T was able to bind TNP-ATP in a similar way to the wild type (data not shown). Displacement of TNP-ATP by ATP was also very similar in both the native and mutant proteins. Thus, the situation is similar to that of P-glycoprotein, in which Lys residues in Walker A, which are critical for catalysis, have no effect on nucleotide binding (18).

DISCUSSION

Relaxosome formation is a relatively well known step in bacterial conjugation, but the subsequent steps remain largely unexplored at the molecular level (11). In this regard, since a coupling protein has been involved in the connection between relaxosome and DNA transport complex (14, 41), it seems that an improved characterization of the coupling protein could shed light on a number of aspects of the conjugation process. However, so far and due to the difficulty in handling integral membrane proteins, almost no data appear in the literature regarding the members of the coupling protein family. TraD protein was the first coupling protein that was purified in its native state and subjected to biochemical analysis (15). As a further step in the study of the coupling protein, we have overproduced and purified TrwB protein to near homogeneity. A remarkable aspect of the purification protocol is the fact that the TrwB monomers and hexamers coexist in the initial membrane preparation and that they can be separated using different elution conditions (Figs. 1 and 2). In a previous work, we purified TrwBΔN70 (11), a truncated form of TrwB that contains only the cytoplasmic domain. Unlike TrwB, TrwBΔN70 behaves as a monomer during purification. In this regard, the hexameric crystal structure of TrwBΔN70 (4, 30) seems to derive from the precipitation conditions. The fact that TrwB, but not TrwBΔN70, forms hexamers in solution indicates that the membrane domain plays a crucial role in the architecture of TrwB and also suggests a dynamic nature for the monomer-hexamer equilibrium.

Electron micrographs of TrwB (Fig. 4) support the data regarding the structure of nonligated TrwBΔN70 shown by Go-

mis-Rüth *et al.* (4, 30). The side view average image is similar, albeit to a different resolution, to the lateral projection of the atomic structure of TrwBΔN70. Nevertheless, although both projections share similar features, at the bottom of the wild-type TrwB, an appendix of ~25 Å wide can be observed, which can be correlated with the transmembrane region of the protein, not present in the structure of TrwBΔN70. The average top view reveals a structure similar to the projection of the atomic structure of TrwBΔN70 along its 6-fold axis. This average image presents, as its atomic counterpart, a central channel and six masses surrounding it, indicating that native TrwB is purified as a hexamer.

TrwBΔN70 has been also crystallized in the presence of nucleotides (4), showing that the nucleotide binding site is localized in the interface between monomers. The nucleotide binding experiments in this work provide TNP-ATP apparent dissociation constants somewhat smaller for the TrwB hexamers ($K_{d(\text{TNP-ATP})}$ = 1.18 μM) than for the monomers ($K_{d(\text{TNP-ATP})}$ = 2.35 μM). In a similar way, when bound TNP-ATP was displaced by ATP, we observed that the TrwB hexamers bound ATP with more affinity than the monomers (apparent dissociation constants 0.48 and 1.20 mM, respectively). Whereas the observed differences are significant, they could not support the idea of inactive half binding-sites that, upon hexamer formation, would complement each other to give fully active binding sites extending over two subunits. Rather, the independent subunits appear to possess active binding sites whose affinity for ATP is only partially increased by hexamerization.

The affinity of TrwBΔN70 for TNP-ATP ($K_{d(\text{TNP-ATP})}$ = 9.20 μM) (11) is lower (by about 10-fold) than the one obtained for TrwB monomers. Therefore, removal of the transmembrane domain affects the nucleotide binding affinity to a higher extent than monomerization itself. This result suggests that the transmembrane domain also plays an important role in stabilization of the cytoplasmic soluble domain of TrwB.

The above results must be interpreted in the light of TrwB being an integral inner membrane protein. This is in agreement with the data from Panicker and Minkley (15) for the cellular localization of TraD (another coupling protein). A model for TrwB function has been proposed in a recent review (2). According to this model, TrwB acts in a second conjugation step, after the conjugative type IV secretion system has achieved transport of the TrwC pilot protein and its trailing DNA. Then TrwB assembles an hexamer in the inner membrane around the transferring DNA and pumps it to the recipient cell. The results of the present work emphasize the dynamic nature of TrwB monomer/hexamer equilibrium in the inner membrane. They also indicate that TrwB ATPase activity, necessary for DNA pumping, requires of an activation step, the nature of which is at present under investigation.

In conclusion, the purification of TrwB in its native form in sufficient amounts for biochemical studies opens the way to a whole series of structural and reconstitution experiments that will shed light on the mechanism of conjugative DNA transfer. With respect to previous studies with truncated forms of TrwB that lack the transmembrane domain, the present data underline the role of such a domain in TrwB hexamerization and ATP binding.

Acknowledgment—We are indebted to Dr. A. Di Pietro (Université Claude Bernard, Lyon) for help with the TNP-ATP binding measurements.

REFERENCES

1. Zechner, E. L., de la Cruz, F., Eisenbrandt, R., Grahn, A. M., Koraimann, G., Lanka, E., Muth, G., Pansegrau, W., Thomas, C. M., Wilkins, B. M., and Zatyka, M. (2000) in *The Horizontal Gene Pool: Bacterial Plasmids and Gene Spread* (Thomas, C. M., ed) pp. 87–173, Harwood Academic Publishers, London
2. Llosa, M., Gomis-Rüth, F. M., Coll, M., and de la Cruz, F. (2002) *Mol. Microbiol.* **45,** 1–8
3. Pansegrau, W., and Lanka, E. (1996) *Progress Nucleic Acids Res. Mol. Biol.* **54,** 197–251
4. Gomis-Rüth, F. X., Moncalián, G., de la Cruz, F., and Coll, M. (2002) *J. Biol. Chem.* **277,** 7556–7566
5. Bolland, S., Llosa, M., Ávila, P., and de la Cruz, F. (1990) *J. Bacteriol.* **172,** 5795–5802
6. Llosa, M., Bolland, S., and de la Cruz, F. (1994) *J. Mol. Biol.* **235,** 448–464
7. Grandoso, G., Llosa, M., Zabala. J. C., and de la Cruz, F. (1994) *Eur. J. Biochem.* **226,** 403–412
8. Llosa, M., Grandoso, G., and de la Cruz, M. (1995) *J. Mol. Biol.* **246,** 54–62
9. Moncalián, G., Grandoso, G. Llosa, M., and de la Cruz, F. (1997) *J. Mol. Biol.* **270,** 188–200
10. Moncalián, G., Valle, M., Valpuesta, J. M., and de la Cruz, F. (1999) *Mol. Microbiol.* **31,** 1643–1652
11. Moncalián, G., Cabezón, E., Alkorta, I., Valle, M., Moro, F., Valpuesta, J. M., Goñi, F. M., and de la Cruz, F. (1999) *J. Biol. Chem.* **274,** 36117–36124
12. Walker, J. E., Saraste, M., Runswick, M. J., and Gay, N. J. (1982) *EMBO J.* **1,** 945–951
13. Lanka, E., and Wilkins, B. M. (1995) *Annu. Rev. Biochem.* **64,** 141–169
14. Cabezón, E., Sastre, J. I., and de la Cruz, F. (1997) *Mol. Gen. Genet.* **254,** 400–406
15. Panicker, M. M., and Minkley, E. G. (1992) *J. Biol. Chem.* **267,** 12761–12766
16. Schröder, G., Krause, S., Zechner, E. L., Traxler, B., Yeo, H-J., Lurz, R., Waksman, G., and Lanka, E. (2002) *J. Bacteriol.* **184,** 2767–2779
17. Thomas, P. J., Garboczi, D. N., and Pedersen, P. (1992) *J. Biol. Chem.* **267,** 20331–20338
18. Lerner-Marmarosh, N., Gimi, K., Urbatsch, I. L., Gros, P., and Senior, A. E. (1999) *J. Biol. Chem.* **274,** 34711–34718
19. Lu, N. T., and Pedersen, P. L. (2000) *Arch. Biochem. Biophys.* **375,** 7–20
20. Ávila, P., Nuñez, B., and de la Cruz, F. (1996) *J. Mol. Biol.* **261,** 135–143
21. Miroux, B., and Walker, J. E. (1996) *J. Mol. Biol.* **260,** 289–298
22. Harlow, E., and Lane, D. (1988) *Antibodies: A Laboratory Manual*, pp. 53–138, Cold Spring Harbor Laboratory, Cold Spring Harbor, New York
23. Osborn, M. J., and Munson, R. (1974) *Methods Enzymol.* **31,** 642–653
24. Cohen, S. N., Chang, A. C. Y., and Hsu, L. (1972) *Proc. Natl. Acad. Sci. U. S. A.* **69,** 2110–2114
25. Marco, S., Chagoyen, M., de la Fraga, L. G., Carazo, J. M., and Carrascosa, J. L. (1996) *Ultramicroscopy* **66,** 5–10
26. Marabini, R., Masegosa, I. M., San Martín, C., Marco, S., Fernández, J. J., de la Fraga, L. G., Vaquerizo, C., and Carazo, J. M. (1996) *J. Struct. Biol.* **116,** 237–240
27. Unser, M, Trus, B. L., and Steven, A. C. (1987) *Ultramicroscopy* **23,** 39–52
28. Hiratsuka, T., and Uchida, K. (1973) *Biochim. Biophys. Acta* **320,** 635–647
29. Grubmeyer, C., and Penefesky, H. S. (1981) *J. Biol. Chem.* **256,** 3718–3727
30. Gomis-Rüth, F. X., Moncalián, G., Pérez-Luque, R., González, A., Cabezón, E., de la Cruz, F., and Coll, M. (2001) *Nature* **409,** 637–641
31. Dupont, Y., Chapron, Y., and Pougeois, R. (1982) *Biochem. Biophys. Res. Commun.* **106,** 1272–1279
32. Watanabe, T., and Inesi, G. (1982) *J. Biol. Chem.* **257,** 11510–11516
33. Divita, G., Goody, R. S., Gautheron, D. C., and Di Pietro, A. (1993) *J. Biol. Chem.* **268,** 13178–13186
34. Conseil, G., Baubichon-Cortay, H., Dayan, G., Jault, J. M., Barron, D., and Di Pietro, A. (1998) *Proc. Natl. Acad. Sci. U. S. A.* **95,** 9831–9836
35. Stewart, R. C., VanBruggen, R., Ellefson, D. D., and Wolfe, A. (1998) *Biochemistry* **37,** 12269–12279
36. Cho, Y-K., Ríos, S. E., Kim, J-J. P., and Miziorko, H. M. (2001) *J. Biol. Chem.* **276,** 12573–12578
37. Garboczi, D. N., Shenbagamurthi, P., Kirk, W., Hullihen, J., and Pedersen, P. (1988) *J. Biol. Chem.* **263,** 812–816
38. Baubichon-Cortay, H., Baggetto, L. G., Dayan, G., and Di Pietro, A. (1994) *J. Biol. Chem.* **269,** 22983–22989
39. Cheng, Y., and Prusoff, W. H. (1973) *Biochem. Pharmacol.* **22,** 3099–3108
40. Mitterauer, T., Nanoff, C., Ahorn, H., Freissmuth, M., and Hohenegger, M. (1999) *Biochem. J.* **342,** 33–39
41. Santini, J. M., and Stanisch, V. A. (1998) *J. Bacteriol.* **180,** 4093–4110
42. Grant, S. G. N., Jesee, J., Bloom, F. R., and Hanahan, D. (1990) *Proc. Natl. Acad. Sci. U. S. A.* **87,** 4645–4649
43. de la Cruz, F., and Grinsted, J. (1982) *J. Bacteriol.* **151,** 223–228
44. Studier, F. W., and Moffatt, B. A. (1986) *J. Mol. Biol.* **189,** 113–130
45. Sandler, J. R., Tecklenburg, M., and Betz, J. L. (1980) *Gene* (*Amst.*) **8,** 279–300
46. Bartolomé, B., Jubete, Y., Martínez, E., and de la Cruz, F. (1991) *Gene* (*Amst.*) **102,** 75–78
47. Stewart, G. S. A. B., Lubinsky-Mink, S., Jackson, C. G., Cassel, A., and Kuhn, J. (1986) *Plasmid* **15,** 172–181
48. Llosa, M., Bolland, S., and de la Cruz, F. (1994) *J. Bacteriol.* **176,** 3210–3217
49. Datta, N., and Hedges, R. W. (1972) *J. Gen. Microbiol.* **72,** 349–355